



Hopf Bifurcations in Electric Power Systems as an impact of high excitation control

Álvaro Augusto Volpato¹

Luís Fernando Costa Alberto²

Department of Electrical and Computer Engineering

São Carlos School of Engineering, São Carlos, SP

Abstract. This paper presents a comprehensive analytical investigation of the Hopf Bifurcation problem associated with high gains of excitation control in Electric Power Systems. The objective is twofold: first, find sufficient conditions for bifurcation in the system, that is, if bifurcation is achievable for a given operating load condition, and second, find bifurcating regions in the space of parameters (controller gains and time constants), finding the combination(s) of parameters that lead the system to Hopf Bifurcation should it be possible. A particular machine model is used to illustrate the results and some implications and discussion follow.

Keywords. Bifurcations, Electric Power System, Transient Stability.

1 Introduction

Synchronous Generators (SGs) comprise the vast majority of generators in modern Electric Power Systems (EPSs). These machines are supplied with mechanical power from a prime mover, usually a turbine, generating a magnetic rotating field through an excitation current on the field windings. Such current is controlled by an Automatic Voltage Generator (AVR), aimed at regulating the machine terminal voltage to a setpoint; despite effective at steady-state conditions, AVR may be harmful to machine transient stability by producing field currents in phase with speed deviation — characterizing the “negative damping” effect. To compensate, a supplementary controller called Power System Stabilizer (PSS) is deployed by adding a signal into the control loop, generating exciter currents acting against speed deviation [2].

While high excitation gains are known to drive the system towards oscillation and instability through the “negative damping” mechanism, they are needed for fast disturbance response and good steady-state voltage regulation. Also, typical design and tuning techniques of these controllers rely on linearized models, providing efficient damping for a

¹alvaro.volpato@usp.br

²lfcualberto@usp.br

limited and narrow range of swing frequencies. However endorsed by several mathematical results when small-scale disturbances are involved, this approach fails to predict complex oscillatory phenomena in the system for its validity is not guaranteed when large disturbances are at play; indeed, controller efficacy is checked *a posteriori* through simulation of the closed loop nonlinear model [4].

Bifurcation events generally occur in over-stressed systems operating on the limits of their power delivery capacity; EPSs are particularly affected as they usually operate in such limits for economical and environmental concerns [1]. Hopf Bifurcations (HBs), particularly, are reported to occur in simple EPS models [5] and even actual power systems [3]; consequently, reserchers have tackled the HB problem associated with high excitation gains, pursuing to foresee and prevent such events; nevertheless, the literature lacks an analytical approach, as numerical and indirect methods are usually employed.

In lieu of such shortcoming, we sought to unravel the One Machine Infinite Bus (OMIB) system in pursue of a closed, analytical form to determine bifurcating regions in the space of parameters. The main contribution is developing a method by which one can determine if such region exists — that is, if there is a combination of parameters that lead the system to bifurcation — and analytically determining such regions by means of parametric investigation, supplying the operator with *a priori* knowledge system stability in the controler design stages, before any numerical simulation is used.

2 Mathematical Background

Nonlinear Autonomous Dynamic Systems (NADSs) are generally represented by a set of Differential-Algebraic Equations (DAEs) as in system (1), where $x \in \mathbb{R}^n$ is the vector of **state variables**, which represent dynamic equations of generators, controllers or loads; $y \in \mathbb{R}^k$ is the vector of **algebraic variables**, generally fruit of applying Kirchoff's Current and Voltage Laws; $\mu \in \mathbb{R}^p$ is the vector of **parameters** such as controller settings and load levels. f and g are supposed C^1 .

$$\begin{cases} \dot{x} = f(x, y, \mu) \\ 0 = g(x, y, \mu) \end{cases} \quad (1)$$

The point (x^*, y^*) is an **equilibrium point** if it satisfies $0 = f(x^*, y^*, \mu) = g(x^*, y^*, \mu)$. If $D_y g(x^*, y^*)$ is invertible, then matrix A , called the **Jacobian of the system** (1) at point (x^*, y^*) , is calculated as:

$$A = \left[D_x f - D_y f (D_y g)^{-1} D_x g \right] \Big|_{(x^*, y^*)}, \text{ where } D_x f(x^*, y^*) = \frac{\partial f}{\partial x} \Big|_{(x^*, y^*)} \quad (2)$$

The eigenvalues of A are called **eigenvalues of the system** at (x^*, y^*) ; according to the Hartmann-Grobman theorem, if all such eigenvalues are hyperbolic (*id est*, all have nonzero real part), then the equilibrium point is asymptotically stable if all are located at the left complex plane; otherwise, the equilibrium is unstable.

If, however, at least one of the eigenvalues of the system is not hyperbolic, nothing can be said about small-signal behavior. So is the case in a Hopf Bifurcation. which occurs for

a critical point μ_B whither a pair of eigenvalues of the system becomes purely imaginary (therefore non-hyperbolic), making linearization-based small-signal analysis around x^* unfeasible.

Also, in order for HB to occur, the *Transversality Condition* (3) requires that the eigenvalues *cross* the imaginary axis in a smooth, continuous fashion.

$$\frac{\partial \lambda(\mu_B, x^*, y^*)}{\partial \mu} \neq 0 \quad (3)$$

3 System Modelling

The target system of this paper is the OMIB system, shown in figure 1, comprised of a SG coupled to an Infinite Bus (a theoretical bus that can absorb or supply any amount of power while maintaining precise voltage levels) through a transmission line.

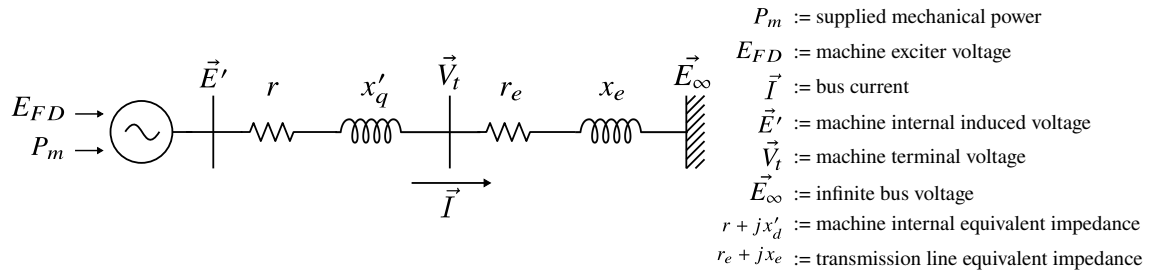


Figure 1: OMIB system schematic circuit.

All phasors are represented not in their imaginary form, but in their QD components which are obtained through Clarke-Park transformation. Equations (4) show the DAEs of the OMIB system of figure 1. Such equations are referred to as One-Axis Model. $E'_q = x_1$ is the quadrature-axis component of induced internal voltage \vec{E}' ; $\omega = x_2$ is the angular speed of the rotor with respect to the QD axis; $\delta = x_3$ is the rotor angle; I_d and I_q are the bus current direct axis and quadrature axis components; H is machine rotor inertia constant, T'_{do} is direct-axis transient time constant, x'_q and x'_d are transient rotor inductances. All of these are constants derived from machine constructive characteristics. Figure 2 shows the closed-loop OMIB system, controlled by both AVR and PSS controllers, and their frequency-space blocks.

$$\begin{cases} \dot{x}_1 = \frac{E_{FD} - x_1 + (x_d - x'_d)\mathbf{I}_d}{T'_{do}} \\ \dot{x}_2 = \frac{P_m - x_1\mathbf{I}_q + (x'_d - x'_q)\mathbf{I}_d\mathbf{I}_q}{2H} \\ \dot{x}_3 = x_2 \end{cases} \quad (4)$$

In order to illustrate the results and conclusions shown in this paper, a particular machine model was used, described by the parameters in (5).

$$\begin{aligned} E_\infty = 1, (x_q, x_d) = (0.66; 1.14), (x'_q, x'_d) = (0.24; 0.24), T'_{do} = 12, H = 1.5, \\ (r_e, x_e) = (0.01; 0.1), (x^*, x_s^*, x_s^*) = (1.115; 0; 0.305 \text{ rad}) \end{aligned} \quad (5)$$

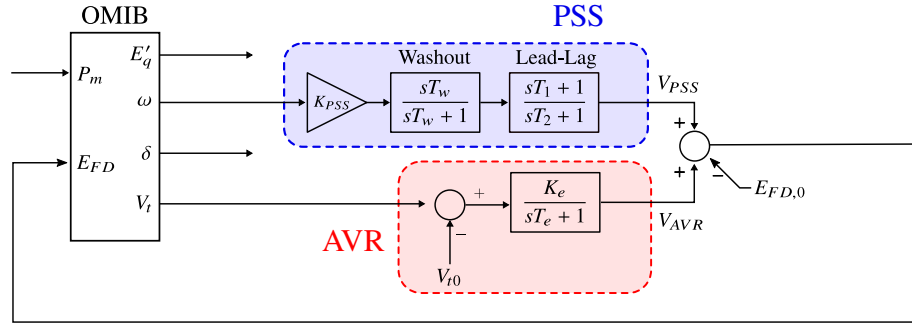


Figure 2: Block diagram of AVR and PSS controlled OMIB system.

4 Hopf Bifurcation in the OMIB system

In order to investigate HB occurrence in the system, one must analytically find the Bifurcation Diagram B_D , the geometric locus of points such that the jacobian matrix of (4) (the system DAEs) $A(x^*, y^*, \mu_B) = A^*(\mu_B)$ has a pair of imaginary eigenvalues:

$$B_D = \{\mu_B \in \mathbb{R}^p : (\exists \alpha \in \mathbb{R}^*) (\det [A^*(\mu_B) - j\alpha I] = 0)\} \quad (6)$$

This is done by forcing $\det [A^*(\mu_B) - j\alpha I] = 0$ and solving for both μ_B and α : let $P(\lambda) = \det [A^*(\mu_B) - \lambda I] = \sum_{i=0}^n a_i \lambda^i$ be the characteristic polynomial of A^* , where the a_i are continuous functions of μ_B^3 and equilibrium x^* . Applying $P(j\alpha) = 0$ and separating imaginary and real parts yields P_{Re} and P_{Im} as in (7).

$$\begin{cases} P_{Re}(\alpha^2) = \sum_{k=0}^{\lfloor \frac{n}{2} \rfloor} (-1)^k a_{(2k)} \alpha^{2k} = 0 \\ P_{Im}(\alpha^2) = \sum_{k=0}^{\lfloor \frac{n-1}{2} \rfloor} (-1)^k a_{(2k+1)} \alpha^{(2k)} = 0 \end{cases} \quad (7)$$

Since $\deg(P_{Im}) \leq \deg(P_{Re})$, if $n \leq 10$ one can analytically solve equation $P_{Im} = 0$ for α^2 in terms of radicals⁴ of μ_B , meaning $\alpha = \alpha(\mu_B)$ is a continuous function⁵ of μ_B and finding an analytical expression for α is achievable.

By substituting the found α into equation $P_{Re} = 0$, then one can solve for μ_B . It is most important to note that, if $P_{Re}(x)$ has only negative roots for every value of μ_B , then no α exists in \mathbb{R}^* meaning $B_D = \emptyset$; therefore that at the particular (x^*, y^*) considered, bifurcation is impossible for any μ value chosen.

³Since the f and g vector fields in (1) are supposed C^1 , then the a_i will be continuous functions of μ_B because they are defined by sums and products of the partial derivatives of those vector fields.

⁴It is needed that $n \leq 10$ because, by the Abel-Ruffini theorem, there is no analytical algebraic solution for quintic roots or any higher degree polynomial.

⁵Because the roots of a polynomial are continuous to its coefficients, which in turn are continuous function of parameter vector μ_B .

4.1 AVR system analysis

In a first moment, the PSS controller is removed from the control loop. The resulting system (AVR-controlled OMIB system) is a fourth-order DAE system hence its characteristic polynomial has degree 4. Computing polynomial P yields $P_{Re}(\alpha^2) = a_1 - \alpha^2 a_3 = 0$ and $P_{Im}(\alpha^2) = a_0 - \alpha^2 a_2 + \alpha^4 a_4 = 0$. Solving the first equation for α gives the value in the left equation of (8); substituting this value onto the latter equation results the right side of (8).

$$\alpha = \sqrt{\frac{a_1}{a_3}} = \sqrt{\frac{\begin{vmatrix} A_{1,1} & A_{1,3} \\ A_{2,1} & A_{2,3} \end{vmatrix} - \frac{A_{2,3}}{\mathbf{T}_e}}{\frac{1}{\mathbf{T}_e} - A_{1,1}}} \Rightarrow 0 = a_0 - \frac{a_1}{a_3} a_2 + \left(\frac{a_1}{a_3}\right)^2 a_4 \quad (8)$$

This equation represents the Bifurcation Diagram (6); by solving it to respect with K_e and T_e one obtains

$$\mathbf{K}_e = \left[\begin{array}{c} \frac{A_{1,3}}{A_{1,4}} \\ A_{1,1} \mathbf{T}_e - 1 \end{array} \right] \frac{\begin{vmatrix} A_{1,3} & A_{1,1} \\ A_{2,3} & A_{2,1} \end{vmatrix} \mathbf{T}_e^3 + A_{2,3} \mathbf{T}_e^2 + A_{1,1} \mathbf{T}_e - 1}{\begin{vmatrix} A_{1,1} & K_{4,1} \\ A_{1,3} & K_{4,3} \end{vmatrix} \mathbf{T}_e - K_{4,3}} \quad (9)$$

Where all $A_{m,n}$ and $K_{m,n}$ are jacobian coefficients that depend only on initial state. Thence for every value of T_e chosen there is a corresponding K_e gain that bifurcates the system; moreover, it can be proven that the left equation of (8) will always yield a real result, meaning bifurcation is possible for any equilibrium point chosen, that is, there will always be a combination (T_e, K_e) that drives the system to bifurcation, despite the equilibrium point or machine parameters.

4.2 PSS-AVR system analysis

When PSS is added to the control loop, the resulting DAE system has order six, significantly hardening the analysis. Solving for α in $P_{Im} = 0$ and substituting in $P_{Re} = 0$ one obtains the results in (10).

$$\alpha = \sqrt{\frac{a_3 \pm \sqrt{a_3^2 - 4a_1 a_5}}{2a_5}} \Rightarrow \Rightarrow 0 = 8a_5^3 a_0 + \left(a_3 \pm \sqrt{a_3^2 - 4a_1 a_5}\right) \left[\left(a_3 + a_5 a_4 \pm \sqrt{a_3^2 - 4a_1 a_5}\right)^2 - a_5^2 (a_4^2 + 4a_2) \right] \quad (10)$$

It can be proven that equation (10) is a sixth-order mixed polynomial on the space of controller parameters, thus while most probably no closed solution exists the equation can be easily solved numerically. By making a small simplification one can determine the existence condition of the upper equation in (10), hence determining if bifurcation is possible: supposing only K_{PSS} and K_e vary, while all controller time parameters remain constant, it can be proven that a_1 and a_3 are given by $a_1 = \alpha_1 K_{PSS} + \beta_1 K_e + \gamma_1$, $a_3 = \alpha_3 K_{PSS} + \beta_3 K_e + \gamma_3$, where all α_i , β_i and γ_i are functions of equilibrium point and time constants. Substituting these onto (10), three independently sufficient conditions arise for bifurcation in the PSS-AVR system:

$$\begin{aligned} \text{(C1)} \quad & (\alpha_1 < 0) \vee (\beta_1 < 0) \vee (\gamma_1 < 0), \quad \text{(C2)} \quad \left[(\beta_1 \alpha_3 - \beta_3 \alpha_1) < 0 \right] \vee \left[(\beta_1 \gamma_3 - \beta_3 \gamma_1) < 0 \right] \\ \text{(C3)} \quad & \left[\beta_3 (\beta_1 \alpha_3 - \beta_3 \alpha_1) > 0 \right] \vee \left[\alpha_3 (\beta_1 \alpha_3 - \beta_3 \alpha_1) < 0 \right] \end{aligned}$$

In other words, by fixing controller time constants, bifurcation is possible if any one of **(C1)**-**(C3)** is true; if so, the exact combination of K_e K_{PSS} that causes bifurcation is found by solving (10).

5 Results and application to test model

The results described in sections 4.1 and 4.2 are then applied to the test model of parameters in (5). For the AVR-controlled system, the Bifurcation Diagram (8) yields figure 3, which describes the controller settings (K_e , T_e) combinations that bifurcate the system.

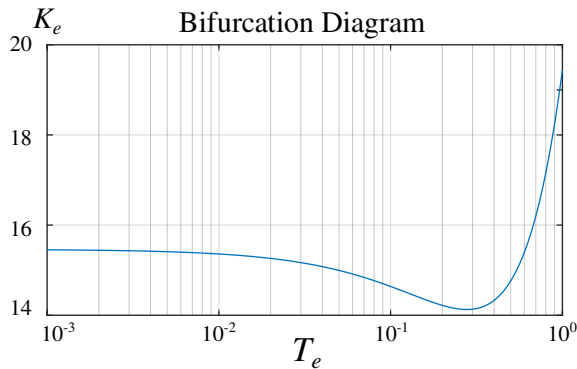


Figure 3: AVR controlled OMIB system Bifurcation Diagram.

Gain values above the line will make the system unstable, while gain values below correspond to stable settings. The graphic shows that there is a minimum gain of approximately 14, below which no gain value is able to drive the system to bifurcation. This suggests that although for any T_e value there is a corresponding bifurcating K_e , keeping the gain value below 14 guarantees that the system will not enter bifurcation. This information is invaluable to the designers and operators, since it provides a well tailored and precise threshold for the controller parameters such that performance is maximized while bifurcation possibility is thwarted.

When PSS is added, time constants (T_1, T_2, T_w, T_e) are fixed to (2, 3, 1, 1) and, according to section 4.2, coefficients a_1 and a_3 can be expressed as $a_1 = 0.03588\mathbf{K}_e + 0.8498$, $a_3 = 0.009195\mathbf{K}_{PSS} + 0.03251\mathbf{K}_e + 3.593$. A close look at these equations will confirm that none of conditions **(C1)**-**(C3)** are met. meaning that for the particular equilibrium point and

time settings chosen, no gain combination (K_e, K_{PSS}) is able to provoke bifurcation; again, this is a paramount information for designers and operators as they are now able to freely adjust gain constants according to performance requirements without the fear of incurring in bifurcation possibility.

6 Conclusion

This paper provides a comprehensive and algorithmic method of precisely calculating controller settings that will lead the OMIB system to Hopf Bifurcation: first, calculate system initial state; then analytically calculate the Jacobian (matrix A) of the system at that equilibrium point. Then impose $\det(A - j\alpha I) = 0$ and thence analyse the possibility of bifurcation through the solutions of $P_{Im}(x) = 0$; in positive case, find bifurcating parameters vector μ_B by solving $P_{Re} = 0$. This enables engineers, designers and operators to obtain *a priori* information about oscillatory phenomena in the system before controller tuning or simulation results, allowing for the possibility of tuning the controllers solely on performance constraints by offering clear gain settings thresholds.

References

- [1] E. H. Abed and P. P. Varaiya Nonlinear oscillations in power systems, International Journal of Electrical Power and Energy Systems, vol.6, 37–43, (1984).
- [2] Francisco P. Demello and Charles Concordia, Concepts of Synchronous Machine Stability as Affected by Excitation Control, IEEE Transactions on Power Apparatus and Systems, n.4, vol PAS-88, 316–329, (1969)
- [3] N. Mithulananthan and S.C. Srivastava, S, Investigation of a voltage collapse incident in Sri Lankan power system network, Proceedings of the International Conference on Energy Management and Power Delivery, vol.1, 47–53, (1998)
- [4] Rodrigo A. Ramos, Stability analysis of power systems considering AVR and PSS output limiters, International Journal of Electrical Power and Energy Systems, n.4, vol. 31, 153–159, (2009).
- [5] Álvaro A. Volpato, Estudos do Impacto de PSSs na Margem de Estabilidade Transitória de Sistemas Elétricos de Potência, Graduation Thesis, University of São Paulo, (2017).